energies

MDPI

Article

Methodology for Sensitivity Analysis of Homogenized Cross-Sections to Instantaneous and Historical Lattice Conditions with Application to AP1000® PWR Lattice

Dean Price [1,*], Thomas Folk [1], Matthew Duschenes [2,3], Krishna Garikipati [2] and Brendan Kochunas [1]

[1] Department of Nuclear Engineering and Radiological Science, University of Michigan, 2355 Bonisteel Blvd., Ann Arbor, MI 48109, USA; thfolk@umich.edu (T.F.); bkochuna@umich.edu (B.K.)
[2] Department of Mechanical Engineering, University of Michigan, 2350 Hayward Ave., Ann Arbor, MI 48109, USA; mduschen@umich.edu (M.D.); krishna@umich.edu (K.G.)
[3] Department of Applied Physics, University of Michigan, 450 Church St., Ann Arbor, MI 48109, USA
* Correspondence: deanrp@umich.edu

Abstract: In the two-step method for nuclear reactor simulation, lattice physics calculations are performed to compute homogenized cross-sections for a variety of burnups and lattice configurations. A nodal code is then used to perform full-core analysis using the pre-calculated homogenized cross-sections. One source of uncertainty introduced in this method is that the lattice configuration or depletion conditions typically do not match a pre-calculated one from the lattice physics simulations. Therefore, some interpolation model must be used to estimate the homogenized cross-sections in the nodal code. This current study provides a methodology for sensitivity analysis to quantify the impact of state variables on the homogenized cross-sections. This methodology also allows for analyses of the historical effect that the state variables have on homogenized cross-sections. An application of this methodology on a lattice for the Westinghouse AP1000® reactor is presented where coolant density, fuel temperature, soluble boron concentration, and control rod insertion are the state variables of interest. The effects of considering the instantaneous values of the state variables, historical values of the state variables, and burnup-averaged values of the state variables are analyzed. Using these methods, it was found that a linear model that only considers the instantaneous and burnup-averaged values of state variables can fail to capture some variations in the homogenized cross-sections.

Keywords: neutronics; MPACT; AP1000®; pressurized water reactor; sensitivity analysis; two-step method; homogenized cross-sections

Citation: Price, D.; Folk, T.; Duschenes, M.; Garikipati, K.; Kochunas, B. Methodology for Sensitivity Analysis of Homogenized Cross-Sections to Instantaneous and Historical Lattice Conditions with Application to AP1000® PWR Lattice. *Energies* **2021**, *14*, 3378. https://doi.org/10.3390/en14123378

Academic Editor: Jong-Il Yun

Received: 5 April 2021
Accepted: 4 June 2021
Published: 8 June 2021

1. Introduction

From the millimeter that may separate the fuel pellet from the cladding to the few meters that may make up the diameter of the core, nuclear reactors contain geometric features that span large scales. As such, techniques such as cross-section homogenization must be used to perform full-scale core design calculations. Homogenization is used to reduce the complexity associated with cross-section dependence on energy and space. Reactor design calculations rely primarily on the "two-step method" [1–3]. The first step consists of independent 2D transport simulations of each lattice. Although some approximations are still made to the lattice geometry/composition at this step (reflective boundary conditions, steady-state operation, cell-wise depletion), the resulting flux solution and homogenized constants can be considered sufficiently accurate to approximate the spatial, and energetic, distribution of the neutron flux in the 3D reactor when combined with generalized equivalence theory. The lattice calculations are often performed with computer codes specifically written to approximate solutions to the neutron transport equation. Often, these codes are coupled with solvers for the Bateman equations [4] such that the change in fuel composition during irradiation is modeled as well. Some

examples of these codes are Serpent [5], TRITON/NEWT [6], POLARIS [6], CASMO-5 [7], MPACT [8], and HELIOS [9], which use a variety of solution methods that may be selected depending on the application. The solutions to the neutron transport equation at multiple states throughout the lattice depletion history are used to generate the homogenized cross-sections (HXS) and diffusion-theory constants (DTC) needed to perform the lower-order full-core calculations. One study which reviews some of the methods used to generate HXS is given in [10]. The second step is to use these data to perform full core analysis using codes such as PARCS [11] or SIMULATE [12].

In the second step of the two-step method, interpolating the HXS/DTC can be non-trivial due to the complexity of the reactor system during burnup. Ref. [13] presents a method for few-group HXS interpolation on sparse grids using multivariate hierarchical interpolation. The method was applied to three different reactor models and a target interpolation accuracy of 0.2% maximum error and 0.05% mean error was achieved for all models for some number of interpolation points. It was observed that introducing grid anisotropy (generating interpolation points along certain dimensions more densely than others) significantly reduced the number of interpolation points to reach the target accuracy. This effect is further explored in [14] where a method for grid-density minimization using perturbation-based approaches is demonstrated for a pressure water reactor (PWR) fuel assembly. The conventional methods for HXS/DTC approximation are multilinear interpolation [15]. Ref. [16] presents a parametric analysis of homogenized cross-sections across operational ranges of burnup, coolant density, coolant temperature, fuel temperature, and boron concentration for a VVER. In addition, a polynomial approximation method using stepwise regression for HXS is demonstrated. A general quasi-regression oriented method for the global approximation of smooth multivariate functions in the context of HXSs is presented in [17]. This method includes the capability to identify—and disregard—insignificant parameters from the regressive model.

One additional complication in the HXS/DTC approximation process is the dependence of these data on the irradiation history of the lattice. Due to the dependence of nuclide composition on neutron spectra during irradiation, two lattices—with the exact same instantaneous configuration/state—can have significant differences in their HXS due to differences in their irradiation histories. Ref. [18] presents a review of methods that can account for these history effects. One approach would be to augment models to account for the past values of state variables. Ref. [19] presents an approach that includes a burnup-weighted average coolant density variable in an HXS model for PWRs. Ref. [20] uses both instantaneous state variables and burnup-weighted average values for multiple state variables. It is clear that these methods add significant computational cost to the lattice simulations because it essentially doubles the parameter space of HXS models. An alternative approach is presented in [18] which uses the “spectral history" of a lattice, or a burnup-weighted average ratio of fast-to-thermal neutron energy flux, as a prediction variable in HXS models. Ref. [21] discusses the importance of history effect modeling, particularly given the desired capacity for the reactor fleet to perform load-follow operation.

The present study presents a new methodology for sensitivity analysis to quantify the effect of not only instantaneous state variables, but also the effect of the past values of these state variables on the HXS. This unique approach provides insight to aid in the parameterization of more complex methods for HXS generation. Previous studies such as [19,20] considered burnup-averaged state variables in HXS models. In this study, a complete state variable history associated with each lattice depletion calculation is incorporated into the sensitivity analysis. The methodology can help provide information on exactly how a particular state variable history can be represented. A lattice-physics code is used to generate HXS for a PWR lattice undergoing a number of random-walks through depletion. A sensitivity analysis is then performed using a form of time-series regression to compute burnup-dependent parametric sensitivities for HXS to instantaneous, historical and burnup-averaged values of the state variables. An application of this methodology on

a 17 × 17 lattice for the Westinghouse AP1000® reactor is presented where coolant density, fuel temperature, boron concentration, and control rod insertion are the state variables of interest. This approach will allow for importance ranking of state variables that can aid analysts in the formulation of models for HXS generation in core simulation. This analysis can aid engineers in developing models for HXS approximation from lattice simulations that may more effectively account for history effects in reactor lattices. With the many advanced reactor designs competing for near-term deployment that may require different parameterization of cross-section models, this methodology can help to identify how to best construct those models. In application to any reactor design, these results can be used to identify the sources of some errors that may arise when using the burnup-averaging methods for HXS approximation.

One useful clarification is that the methods presented in this paper are not intended to act as a sensitivity analysis *in the context of uncertainty quantification.* Although ranges of input parameters are specified, these ranges correspond to hypothetical operational ranges of a nuclear reactor for which some HXS prediction model should be valid over. In studies focused on uncertainty quantification, ranges of input variables can be specified which represent the possible values of some input parameter given an estimation of its value. In uncertainty quantification, sensitivity analysis is typically performed for much narrower input domains than those used in this study. Currently, there is a multi-institutional effort to further explore uncertainties introduced in the two-step method due to nuclear data and operational data uncertainties [22]. This effort, the Benchmark for Uncertainty Analysis and Design (UAM), involves the use of both sampling and direct-perturbation based approaches to uncertainty propagation for final result analysis in core simulation codes. This benchmark is a good source for information for sensitivity analysis in the context of uncertainty quantification. In the current work, the sensitivity analysis is presented with respect to some realistic operational ranges of state variables that could be said to be known, not uncertain, parameters.

2. Methods and Models

This section is divided into three subsections, and the first provides some of the details and methods used to simulate the depletion of the PWR lattice model. Following this, a subsection is given on the structure of depletion calculations necessary to perform this analysis. Finally, a formulation of the sensitivity analysis method is presented.

2.1. Lattice Model

The lattice model used to perform the study is based on a 17 × 17 lattice from the Westinghouse AP1000® reactor. Referred to in [23] as "Region B", a pin map of the lattice with 1/8th symmetry is given in Figure 1. The lattice contains 264 UO_2 fuel rods with a uniform enrichment of 1.58% U-235 and ZIRLO® cladding. This lattice was selected because it is thought to represent the most simple lattice design that may be used in a PWR. In more complex lattice designs, there may be higher or lower sensitivities to the various state variables during burnup. There are 24 guide tubes that are either modeled with B_4C control rod inserts or filled with water depending on the lattice state being modeled. There is also a single instrumentation tube in the center of the lattice that remains filled with water in all lattice configurations explored in this study. In terms of geometry, the pin pitch of the lattice is 1.26 cm. The fuel pellet inner radius is modeled to be 0.418 cm and in contact with the inner surface of the cladding. The cladding outer radius is 0.475 cm, and the guide tube and instrumentation tube have inner and outer radii of 0.561 cm and 0.612 cm, respectively.

For HXS generation of the lattice, the neutronics code MPACT [8,24] is used. MPACT is a neutron transport code based on the method of characteristics that was developed at the University of Michigan for use in the reactor simulation tool VERA (Virtual Reactor Environment for Reactor Analysis) [25] and is now jointly developed by the University of Michigan and Oak Ridge National Laboratory.For this study, burnup calculations are

performed with 51 energy groups for a PWR lattice. The ENDF/B-VII.1 nuclear data library was used.

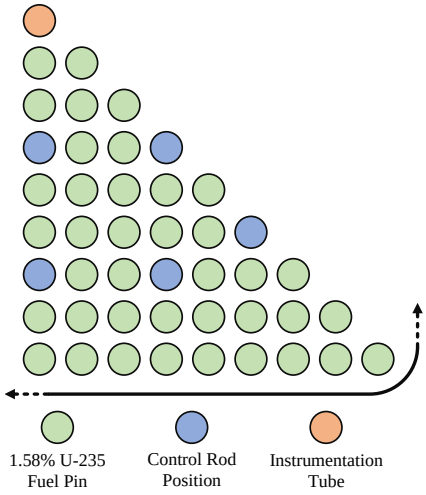

Figure 1. Radial pin layout of AP1000® Region B Lattice.

2.2. Sampling Approach

A random-sampling based approach is used to generate the dataset for the sensitivity analysis. Four state variables are selected:

- coolant density;
- fuel temperature;
- boron concentration in coolant;
- control rod insertion.

For any coolant density incorporated into a model, a corresponding coolant temperature will be used according to the isobaric properties of water at a pressure of 15.5 MPa. These parameters were selected both because they are known to have a large effect on lattice characteristics, and they are commonly used in other studies [13,26,27]. However, this methodology is certainly general and scalable enough to include any number of other lattice parameters providing there is the computational capability to generate a sufficient number of samples and those lattice parameters have a reasonably linear relationship with the homogenized cross-sections.

It is well known in the community that the Doppler-coefficient—which describes the effect on HXS from changes in fuel temperature—varies linearly with the square root of the fuel temperature [28]. The methodology used in this study relies on linearity in the relationships between the HXS and state variables for both the values of the state variables at which the HXS is calculated as well as past values of the state variables leading up to the state for which the HXS is calculated. It is expected that the relationship between the *historical* values of fuel temperature, and HXS is not necessarily more linear with respect to the square root of the fuel temperature than with respect to fuel temperature alone. Therefore, it was decided that the fuel temperature, without the square root, will be used for this analysis. Work was done to ensure that, in the range of fuel temperatures used for analysis, the linear models based on the fuel temperature performed comparatively to linear models based on the square root of the fuel temperature.

In this context, the building blocks for the sampling process are single lattice burnup sequences. For constant burnup spacing in each history, a new set of state variables are independently selected according to their distributions listed in Table 1. In order to obtain accurate results for the state variable history considered, substeps may be taken in the burnup calculation where the lattice does not change state, but the Boltzman and Bateman equations are still solved. In other studies for HXS construction, there may be branch states considered from each burnup state, but, in this study, none are considered because a full

lattice history is sampled. Figure 2 is included to give the reader an understanding of the structure of the burnup sequence. Figure 2a shows the progression of fuel temperature and coolant temperature of a single lattice through a potential burnup sequence. Boron concentration and control rod insertion are not shown. Blue points depict states where HXS are calculated, and they are intentionally placed after burnup at state $\vec{x}$ and before the transition to the next state. It is expected that, for a short time after a transition, the lattice may undergo nontrivial changes in its fuel composition as it adjusts to the new neutron energy spectrum. By calculating HXS at the the end of these periods, instead of the beginning, it is thought that a more representative HXS for the fuel composition of that burnup during the segment will be obtained. Solid blue lines show depletion states, and dashed lines show transitions from the current depletion state to the next sampled state. Figure 2b shows the structure of the burnup sequences and some mathematical notation that will be used in Section 2.3. A state vector, denoted by $\vec{x}_n$, is composed of values of state parameters at burnup point n. The state vector is fixed during some burnup period ΔB. BU_n will be used to indicate the value of the burnup at the end of increment n. Following the lattice depletion calculation reaching burnup increments of ΔB, a new $\vec{x}_n$ is independently sampled according to the distribution of its components. In this application, the four parameters given in Table 1 are used. In this study, the ranges were chosen to reflect a wide range of possible operating conditions to explore the extent of the linearity in the relationship between the state variables and the HXS for an exaggerated range of operating conditions. One practical consideration is that, in realistic operation, fuel temperature is closely related to reactor power, which in turn is related to burnup. This leads to an interaction between T_f and burnup that is not considered in this sampling approach. In addition, there are no covariances considered in the sampling process so sampled state values may not reflect realistic operational conditions. However, given the strong linear relationships observed between these state variables and the HXS, the results obtained for this wider domain should be applicable to any other domain that one may find to be realistic given that it falls within the operational ranges specified. In specific applications, care should be taken to ensure that these ranges are appropriate. In datasets where some state variables are held constant, they are held at the value in the "Nominal Value" column of the table.

In these results, a ΔB of 3 GW/MTU is used up to a maximum burnup of 60 GWD/MTU. For low burnups, 1 GWD/MTU substeps are taken where the reactor state does not undergo any parametric transition, but the code still calculates the change in fuel composition. Although in practical scenarios it is unlikely that a lattice would frequently undergo such radical changes in its operational state, this approach allows for a more flexible methodology that can generate sensitivities for any lattice independent of operational data availability.

Table 1. State variable distributions independently sampled in each burnup step.

State Variable	Notation	Distribution	Distribution Specs.	Nominal Value	Unit
Coolant Density	ρ	Uniform	[min = 0.652, max = 1.01]	0.712	g/cm^3
Fuel Temperature	T_f	Uniform	[min = 293, max = 1793]	900	K
Boron Concentration	b	Uniform	[min = 0, max = 3000]	800	ppm
Control Rod Insertion	r	Bernoulli	[50% in/out]	out	

In Section 2.3, a method for the sensitivity analysis is described which relies on burnup-averaged values of the state variables as independent parameters for analysis. This leads to distributions of burnup-averaged values that have lower variances than the instantaneous distributions of those parameters. This effect is formally described by the central limit theorem. In the end, scenarios with some nonlinearities may result in biased estimates for the global sensitivity. This study sought to maintain the number of burnup levels at a reasonably low level to minimize this effect.

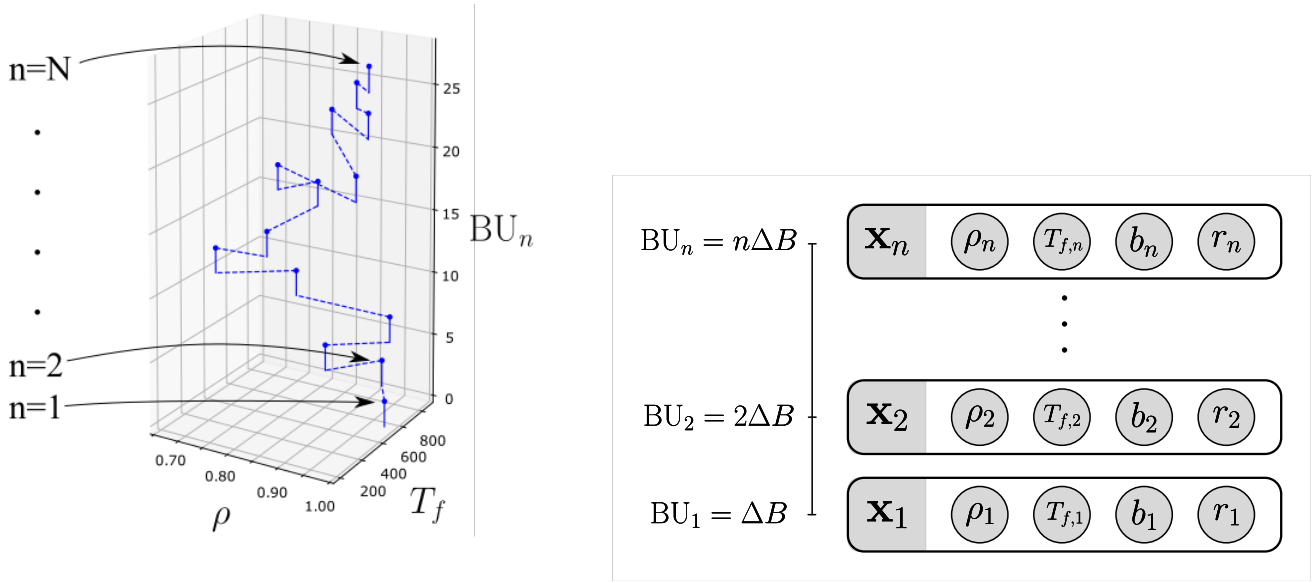

(**a**) (**b**)

Figure 2. Structure of burnup sequences. (**a**) depiction of coolant temperature and fuel temperature change over burnup for a single burnup sequence sample; (**b**) structure of state vectors and evolution through burnup. Each component of $\vec{x}$ is independently sampled from their respective distributions.

2.3. Sensitivity Analysis

Here, a description of the method for sensitivity quantification for the effect of both instantaneous and historical values of state variables on HXS. In this context, burnup is not used as a lattice state variable and is instead treated similarly to the temporal axis in conventional time-series analysis. Some general HXS, denoted as Σ_n at burnup set n, is calculated with a physics-based computer simulation and can be written as some explicit function of the instantaneous value of the state vector as well as all historical values of the state vectors during burnup as is shown in Equation (1). In this equation, $\vec{x}$ refers to a vector of state variables, with the subscript referring to which burnup step in the simulation those state variables correspond to. For example, if the boron concentration in the coolant and fuel temperature are the two state variables for which sensitivities are to be computed, $\vec{x}_1 = [2000 \text{ ppm}, 600 \text{ K}]$ if the reactor can be approximated to have a boron concentration of 2000 ppm and a fuel temperature of 600 K at the first portion of the cycle. Throughout this paper, the instantaneous state vector will refer to the state vector which describes the reactor state at the time in which the HXS is calculated. For now, notation indicating reaction type in Σ will be forgone:

$$\Sigma_n = f(\vec{x}_n, \vec{x}_{n-1}, ..., \vec{x}_1). \tag{1}$$

It is the aim of the methods described in [13–16,18,21] to best approximate f using reduced-order methods based on the pre-calculated relationships between Σ and $\vec{x}$. This is not the aim of our current study. Instead, as a sensitivity study, the gradient of Σ_n is the quantity of interest, as shown in Equation (2). The exact form of the gradient operator will be described in more detail later in this section; however, its form is given in Equation (10):

$$\nabla\Sigma_n = \nabla f(\vec{x}_n, \vec{x}_{n-1}, ..., \vec{x}_1), \tag{2}$$

From here, an approximate linear model for Σ can be written according to Equation (3). $\hat{\Sigma}$ denotes an estimated value of Σ. The subscript on $\hat{\Sigma}$ functions identically to the subscript on Σ, and it describes the burnup step. The vector $\boldsymbol{\beta}$ and scalar α are fitted model parameters estimated using ordinary least squares (OLS). The subscripts on each $\boldsymbol{\beta}$ indicate how many burnup steps back in the history from n a set of fitted coefficients correspond to. α does not

have any subscript because there will only be one fitted α parameter for any model used to predict $\hat{\Sigma}_n$. Full physics-code calculations will be performed to get data to perform this fit. Proceeding forward, this model will be referred to as the complete history model (CHM). This name is assigned because the expression for $\hat{\Sigma}_n$ contains all reactor states present in the history of the reactor. No averaging is performed across multiple states in the history. The origin of the model is assumed to be that the homogenized cross-section is a linear function of each state variable at each burnup step across the entire history. The fitting calculation will be demonstrated later in this section:

$$\hat{\Sigma}_n = \alpha + \sum_{j=0}^{n-1} \boldsymbol{\beta}_j^T \vec{x}_{n-j}, \tag{3}$$

Although the previous formulation can lead to sensitivity estimates for every state parameter for every burnup step leading to state n, the number of fitted parameters becomes very large. An alternative model, featuring some model reduction parameter Q, can be used to include burnup-weighted average state vectors. This model will be referred to as the reduced history model (RHM). In this model, a fitted vector, $\boldsymbol{\gamma}$, is used to capture the effect from the historical values of the state vector for previous steps greater than Q without assigning fitted parameters to each of these historic states individually. $\boldsymbol{\gamma}$ is assigned to the historic average of these state variables. Q can be selected to balance the interpretability and precision of the results. Higher Q values will result in sensitivity measures for the state variable values for more states in a burnup sequence to be reported. Lower Q values will provide less sensitivity measures by averaging the initial portions of the burnup sequence. Instead, the averages of these historic states are used. The equation for the RHM is shown in Equation (4). This equation can be obtained by considering a state vector that is the element-wise average of all state vectors in the history greater than Q steps back. This new state vector is also assigned a vector of fitted parameters. For this equation, there are two limiting cases worth mentioning:

- $Q = n - 2$: This is the largest allowable value for Q. In this case, the RHM and CHM become identical in that the fitted $\boldsymbol{\gamma}$ parameter operates on the single $\vec{x}_1$, functioning identically as $\boldsymbol{\beta}_{n-1}$ in the CHM.
- $Q = 0$: This is the smallest possible value for Q. In this case, only the current value of the state vector $\vec{x}_n$ is assigned an individual fitted vector. The remaining state vectors are averaged and assigned a single fitted vector:

$$\hat{\Sigma}_{n,Q} = \alpha + \sum_{j=0}^{Q} \boldsymbol{\beta}_j^T \vec{x}_{n-j} + \boldsymbol{\gamma}^T \frac{1}{n-Q-1} \sum_{j=Q+1}^{n-1} \vec{x}_{n-j} \quad \text{for} \quad 0 \le Q < n-1, \tag{4}$$

In order to fit the RHM model, OLS is used with a number of sampled burnup sequences. Each burnup sequence yields N relationships between HXS and historical and instantaneous values of the state vectors, where N is the total number of burnup steps in the sequence. A linear system of equations can be formulated according to Equation (5). This equation is used to estimate the linear model parameters. Here, $\vec{x}_n^{(i)}$ is the state vector at burnup step n in burnup sequence i and $\Sigma_n^{(i)}$ is the computed homogenized cross-section at burnup step n for burnup sequence i. The goal of the OLS fit is to find some optimal set of linear model parameters that best predicts the result vector $\vec{y}_n$. Therefore, there are no superscripts on the α and $\boldsymbol{\beta}$ fitted parameters because they will have the same values across all sampled burnup sequences. I is the total number of burnup sequences generated by the lattice physics code. This can be understood as the specific number of realized operational histories that get randomly sampled. The subscripts on the matrices are used to indicate the values of n and Q that can be used to form the matrices.

$$\vec{X}_{n,Q} \boldsymbol{\lambda}_{n,Q} = \vec{y}_n \quad , \tag{5}$$

where

$$\vec{X}_{n,Q} = \begin{bmatrix} 1 & \vec{x}_n^{(0)} & \vec{x}_{n-1}^{(0)} & \cdots & \vec{x}_{n-Q}^{(0)} & \frac{1}{n-Q-1}\sum_{j=Q+1}^{n-1}\vec{x}_{n-j}^{(0)} \\ 1 & \vec{x}_n^{(1)} & \vec{x}_{n-1}^{(1)} & \cdots & \vec{x}_{n-Q}^{(1)} & \frac{1}{n-Q-1}\sum_{j=Q+1}^{n-1}\vec{x}_{n-j}^{(1)} \\ \vdots & \vdots & \vdots & & \vdots & \vdots \\ 1 & \vec{x}_n^{(I)} & \vec{x}_{n-1}^{(I)} & \cdots & \vec{x}_{n-Q}^{(I)} & \frac{1}{n-Q-1}\sum_{j=Q+1}^{n-1}\vec{x}_{n-j}^{(I)} \end{bmatrix},$$

$$\boldsymbol{\lambda}_{n,Q} = \begin{bmatrix} \alpha & \boldsymbol{\beta}_0 & \boldsymbol{\beta}_1 & \cdots & \boldsymbol{\beta}_Q & \gamma \end{bmatrix}^T,$$

$$\vec{y}_n = \begin{bmatrix} \Sigma_n^{(0)} & \Sigma_n^{(1)} & \cdots & \Sigma_n^{(I)} \end{bmatrix}^T.$$

With this formulation, the fitted model parameters can be found using the normal equations according to Equation (6). The total number of fitted parameters (including the individual components of $\boldsymbol{\beta}$ and γ) in $\boldsymbol{\lambda}_{n,Q}$ for these models is $1 + (Q+2)P$; therefore, for large Q, there is a need for a large number of sampled burnup histories to get an adequate estimate for $\boldsymbol{\lambda}_{n,Q}$. However, as mentioned previously, an estimate for the sensitivity is the true desired quantity of interest that may help inform the creation of more accurate surrogate models for HXS interpolation:

$$\boldsymbol{\lambda}_{n,Q} = (\vec{X}_{n,Q}^T \vec{X}_{n,Q})^{-1} \vec{X}_{n,Q}^T \vec{y}_n, \tag{6}$$

Furthermore, this model can only capture linear relationships between the state variables and the HXS. The validity of this assumption will be explored later in this study in Section 3. One useful definition for linear model evaluation is the coefficient of determination, often referred to as R^2. This quantity describes the fraction of variance in the result that can be explained by the model and can be calculated using Equation (7), where the definition for $\overline{\Sigma}_n$ is simply the HXS averaged across all burnup sequences at step n. Here, the subscripts of n and Q are maintained to indicate the form of model that corresponds to some computed R^2:

$$R_{n,Q}^2 = 1 - \frac{\sum_{i=0}^{I}\left(\Sigma_n^{(i)} - \hat{\Sigma}_{n,Q}^{(i)}\right)^2}{\sum_{i=0}^{I}\left(\Sigma_n^{(i)} - \overline{\Sigma}_n\right)^2}, \tag{7}$$

Moving on, one important technique used in sensitivity analysis is "data standardization". This is a linear transformation which scales the mean and variance of the input and output parameter distributions to 0 and 1, respectively. This has the benefit of non-dimensionalizing the data according to the range of its variation. After fitting the linear model, the resulting sensitivity measures will account for both the magnitude of impact a particular state variable has on the HXS as well as the range of variation of that parameter. Formally, this is often referred to as the standardized regression coefficient method [29] for sensitivity analysis. Often in statistical analysis, one of the first steps is for the analyst to standardize the data. However, in this application, the standardization transformation should only be performed after the formation of the $\vec{X}_{n,Q}$ matrix where each column should be standardized. As mentioned previously, by performing burnup-averaging, the distributions of the parameters in the linear models are changed. By standardizing the columns of $\vec{X}_{n,Q}$, it ensures that the standardization transformation is applied after the narrowing of the burnup-averaged state variable distributions has occurred. Furthermore, this transformation loses its usefulness if applied to binary state variables, such as control rod insertion. Nevertheless, to perform this transformation on $\vec{y}_n$, Equation (8) can be used. Here, the mean of the elements in $\vec{y}_n$ ($\overline{y}_n$) at burnup step n is subtracted and then this quantity is further divided by the standard deviation (s_{yn}) to yield the normalized vector $\vec{y}_n'$. An identical operation can be preformed column-wise on $\vec{X}_{n,Q}$ according to

Equation (9). Here, $\vec{X}_{n,Q}(r,c)$ indicates the element in $\vec{X}_{n,Q}$ that corresponds to row r and column c, $\overline{X}_c$ denotes the average of column c of $\vec{X}_{n,Q}$, $s_{x,c}$ denotes the standard deviation of column c of $\vec{X}_{n,Q}$, and $\vec{X}'_{n,Q}$ refers to the column-standardized form of $\vec{X}_{n,Q}$:

$$\vec{y}'_n = \frac{\vec{y}_n - \overline{y}_n}{s_{yn}}, \tag{8}$$

$$\vec{X}'_{n,Q}(r,c) = \frac{\vec{X}_{n,Q}(r,c) - \overline{X}_c}{s_{x,c}}, \tag{9}$$

To compute sensitivities for the model form given in Equation (4), an expression for ∇ is needed. This is given in Equation (10), which yields a measure of the sensitivity of the HXS to the desired parameters. This sensitivity estimate will be global with respect to the various state parameters but local to the burnup step n; hence, the subscript on each of the derivatives:

$$\nabla_{n,Q} = \left[\begin{array}{ccccc} \frac{\partial}{\partial \vec{x}_n} & \frac{\partial}{\partial \vec{x}_{n-1}} & \cdots & \frac{\partial}{\partial \vec{x}_{n-Q}} & \sum_{j=Q+1}^{n} \frac{\partial}{\partial \vec{x}_{n-j}} \end{array} \right]^T, \tag{10}$$

If this gradient operator is applied to the linear model given in Equation (4), the result vector is given in Equation (11). Here, the subscripts on the ∇ can be inferred from the subscripts on $\hat{\Sigma}_{n,Q}$. This form provides a clear mathematical definition for the sensitivity coefficients used in this study. If the standardization transformation is performed on $\vec{X}$ and $\vec{y}$, $\nabla\hat{\Sigma}_{n,Q}$ aligns with the definition for sensitivity measures from the standardized regression coefficient (SRC) method [29] where instantaneous, historical, and burnup-averaged state variables are considered parameters of interest. To explain further, without the standardization transformation, the fitted linear model coefficients can be interpreted as the change in HXS for some unit change in the state variable. Although this sensitivity measure may be useful in many analyses, if the goal is to compare the sensitivities of *different* state variables, these coefficients are not as useful. At the simplest level, some state variables will have different units because they represent different quantities, making a comparison between those values meaningless. However, the more fundamental problem is that these state variables may have wildly different ranges of variation that will not be accounted for. For example, in more generalized applications, if two parameters have the same unit and vary at different orders of magnitude, it is possible that, despite having the same dimensionalized sensitivity coefficient, the outcome of the system is significantly more influenced by the parameter with the larger range of variation. The standardization transformation scales the ranges of all parameters to be unity, which allows for the magnitude of influence as well as the range of variability to be accounted for in a single sensitivity measure:

$$\nabla\hat{\Sigma}_{n,Q} = \left[\begin{array}{ccccc} \beta_0 & \beta_1 & \cdots & \beta_Q & \gamma \end{array} \right]^T, \tag{11}$$

To summarize the two models used for sensitivity analysis:

- Full History Model (FHM): Uses every reactor state variable in the history leading up to the burnup at which the HXS is calculated to calculate sensitivities.
- Reduced History Model (RHM): Uses a reduction parameter to use burnup-averaged state variable values instead of considering the reactor state at every burnup step.

2.4. Workflow Summary

This section will help to summarize the previous content and provide a logical progression for how a sensitivity analysis following the proposed methodology can be performed. Mainly, the discussion will be centered around the flow chart provided in Figure 3. To begin, the ranges and distributions of the state variables used in the analysis should be carefully considered. These ranges should cover the reasonable ranges for the reactor in some specific application and no more. Wider operational ranges lead to weaker linearity between state variables and HXS. Separate analysis can be done for multiple application

states, but including these operational ranges in an analysis intended for an operating reactor can skew the reported sensitivities to reflect undesired states. Following this, burnup sequences should be sampled according to these distributions. This sampling is represented by the "Burnup Sequence Sampling" box in the flowchart. These processes are described in more detail in Section 2.2. The result of this sampling procedure is represented by the "Data" boxes containing $\vec{x}_n^{(i)}, \vec{x}_{n-1}^{(i)}, ..., \vec{x}_1^{(i)}$. Here, the subscripts indicate the burnup step that the state vector $\vec{x}$ corresponds to. The superscript i indicates which of the I total samples the burnup sequence corresponds to.

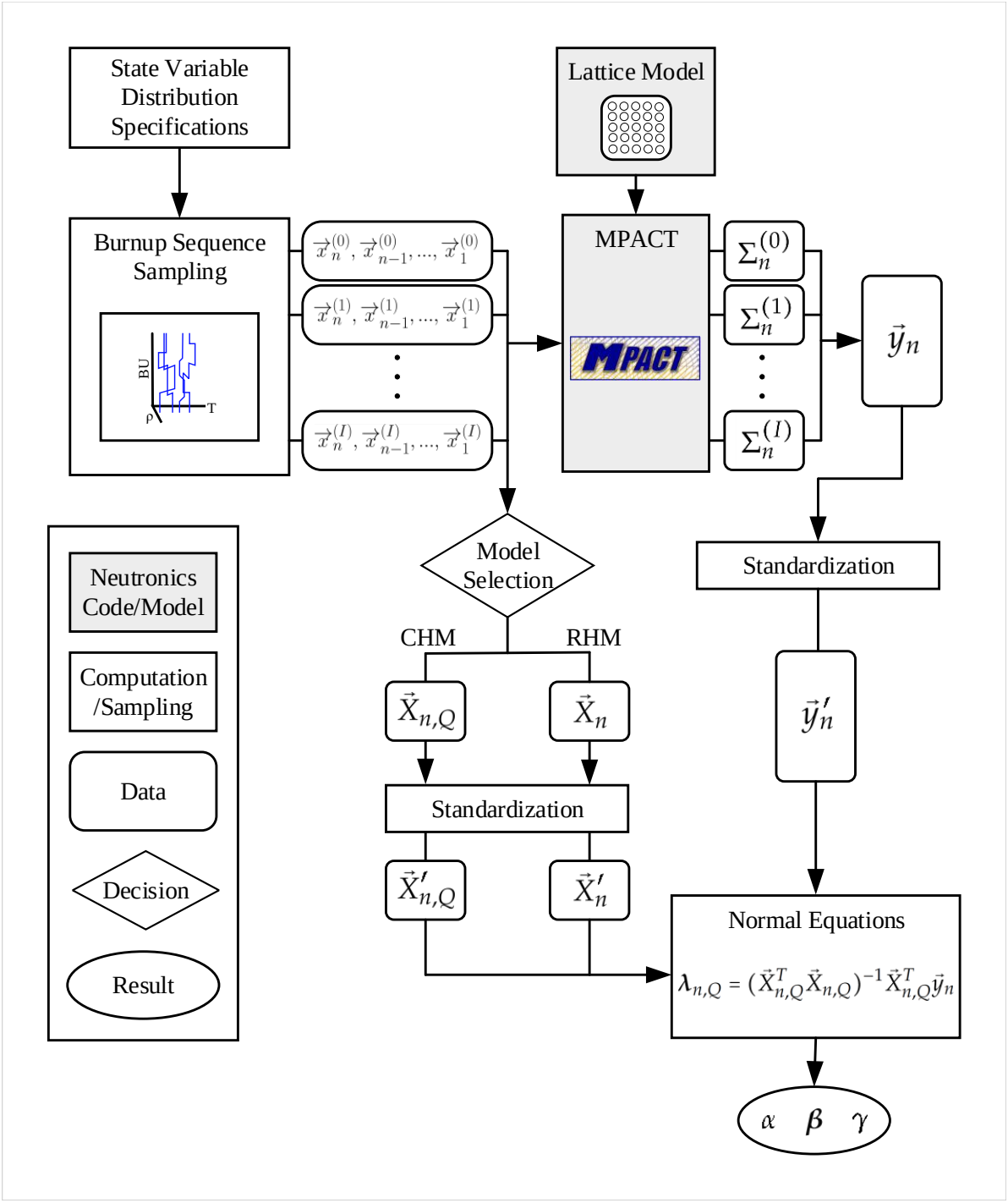

Figure 3. Potential workflow to execute the proposed methodology to obtain sensitivity estimates for some HXS at some burnup step n.

Moving on with the burnup sequences, an MPACT depletion calculation must be performed on each sample. Of course, the lattice geometry and materials must also be provided for this calculation to be performed—as indicated by the box titled "Lattice Model". The result of these calculations is a series HXSs at burnup step n for each sample i, denoted as $\Sigma_n^{(i)}$. This analysis can be performed with any HXS so the reaction type is neglected in the notation. The set of HXS can then be compiled into the vector $\vec{y}_n$ as described by Equation (5).

Separately from the MPACT calculations, the $\vec{X}$ matrices can be formed directly from the sampled burnup sequences as described in Equation (5). Prior to this formation, however, the analyst must first select whether the CHM or RHM will be used—as indicated by the "Decision" diamond labeled "Model Selection" in Figure 3. This decision should be made based on the complexity of the desired result. For a complete understanding of the sensitivity of an HXS to every historic value of a state variable, the CHM should be used. For more interpretable results, smaller values of Q can be used for the RHM. The formation of the $\vec{X}$ matrix in the case of the CHM is identical to the RHM case where $Q = n - 2$.

From here, both $\vec{X}_{n,Q}$ and $\vec{y}_n$ can be standardized according to Equations (8) and (9). With the standardized versions of these quantities, the normal equations can be solved to obtain $\boldsymbol{\lambda}_{n,Q}$. From Equation (5), it can be seen that $\boldsymbol{\lambda}_{n,Q}$ is composed of the sensitivity measures that align with the definition from Equation (11) that can be used for further analysis.

3. Model Evaluation

One important step in applying this methodology to any reactor system is assessing the validity of the CHM and RHM models *in their use for computing sensitivities for the range of parameters used* . It can be seen in existing literature that the relationships between the various state variables and the HXS can be nonlinear [14,16]; this is why many of the aforementioned studies use more complex models for HXS generation that can account for these nonlinearities. Although the models used in this study cannot account for these nonlinearities, the formulation of the model allows for clear estimates of sensitivities over the concerned range after the gradient operator given in Equation (10) is applied. The linear nature of the models used in this study allows for the gradient to be constant across the domain of interest. Therefore, the models presented in this study are not intended to act directly as models for HXS generation and should instead be used to estimate sensitivities that can inform the creation of other models that can be used for HXS generation. Furthermore, given that the sensitivity estimates are global with respect to the state variables, it would be useful to evaluate the extent that local sensitivity estimates may significantly deviate from global approximations. Table 2 gives the coefficient of determination, as described in Equation (7), when fitting the CHM to predict various HXS in the final burnup considered at 60 GWD/MTU. This burnup was selected because it may be representative of the performance of this method for higher burnups, which may be more difficult to predict due to the generation of assorted actinides and fission products that depend on past states of the lattice. Although not shown here, the R^2 values do not change significantly for lower burnups. Five different datasets are used, each composed of burnup sequences with sampled state parameters given in Table 1. For each dataset, there is a different set of state parameters that are perturbed, each according to the distributions given in Table 1. Three datasets vary for a single parameter: coolant density, fuel temperature, or boron concentration are each varied for 150 samples. One dataset varies coolant density, fuel temperature, and boron concentration simultaneously for 550 samples. The final dataset has all state parameters varied simultaneously for 400 samples. State parameters that are not varied are held at their nominal values. R^2 values suggest that the variability in all four of the HXS shown can be largely explained by the model for all datasets. The coefficient of determination can increase as more varied parameters are added (as is the case for $\Sigma_{f,2}$) because the linearity in the relationships of these additional parameters can overshadow nonlinear relationships with those original state variables. To explain, consider a slightly nonlinear relationship between some state

variable and an HXS. If a coefficient of determination were to be computed to describe the relationship between this state variable and the HXS, it would be low, indicating a weak linear relationship between the two variables. If a largely influential parameter with a linear relationship with the HXS is then added, the relationship described by R^2 will be be completely dominated by this new variable with strong linearity. Hence, the linearity arising from this new parameter will increase R^2, overshadowing the nonlinear relationship with the original variable.

Table 2. Coefficient of determination using the CHM to fit to burnup sequence datasets with different varying state variables for the final burnup considered at 60 GWD/MTU. Checkmarks indicate varied state variables for each data set. *I* indicates the number of samples in the dataset.

I	ρ	T_f	b	r	$\Sigma_{f,1}$	$\Sigma_{f,2}$	$\Sigma_{rm,1}$	$\Sigma_{rm,2}$
150	✓				0.989	0.799	1.000	0.956
150		✓			0.995	0.997	0.984	0.997
150			✓		0.999	0.998	0.999	0.999
550	✓	✓	✓		0.989	0.970	1.000	0.973
400	✓	✓	✓	✓	0.982	0.974	0.999	0.992

As previously mentioned, the CHM contains a large number of parameters where a sensitivity estimate for each parameter may not be needed. In addition, having sensitivity estimates for such a large number of parameters can lead to less-interpretable results. As such, the RHM can be used to characterize the relationship between the state variables and the HXS and yields a lower number of sensitivity estimates. Figure 4 gives R^2 values for both energy groups of the homogenized fission cross-section for the lattice. The removal cross-section is not included because all R^2 values are above 0.98 with trends that will be discussed in later sections. A variety of RHMs are used with different Q and n values, the dataset with all state parameters varied, and 400 samples are being used. In this figure, BU_n is the x-axis which corresponds to the burnup at n. Each line in this figure corresponds to models with the same Q applied to different values of n. Models are shown with all possible Q values (up to Q = 18), but, for clarity, only lines up to Q = 4 are labeled. As n increases with burnup, the $Q < n - 1$ relationship allows for models to be created with higher Q values.

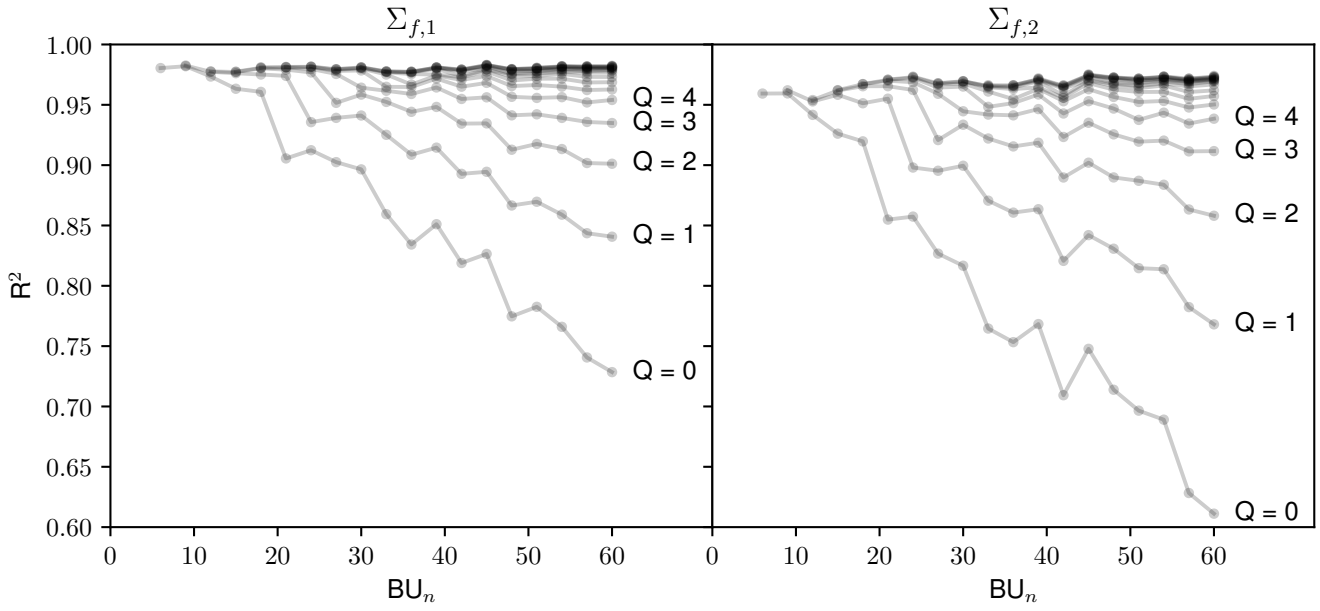

Figure 4. Coefficient of determination for varying Q values when fitting the RHM to the relationship between all state variables and fission HXS over all burnups.

From Figure 4, the RHM can fit the trends in the fission HXS for the fast ($\Sigma_{f,1}$) and thermal ($\Sigma_{f,2}$) groups given a sufficiently high Q parameter. For each of the constant-Q lines, the burnup at which the line starts corresponds to $Q = n - 2$. This is where the CHM and RHM are identical. As n increases, the past state vector behavior for burnups less than $((n - Q - 1)\Delta B)$ is averaged, reducing the detail of the model. Hence, the R^2 of the model will decrease. These results demonstrate that some HXS prediction methods that rely strictly on the instantaneous values of the state variables and burnup-averaged quantities may fail to account for the effects of state variable changes over burnup. The explanation for this is the complex relationship between the production of fission products/consumption of fissile isotopes and neutron flux distribution in space and energy that results from the coupled Boltzman and Bateman equations. Methods that average burnup-dependent quantities may fail to account for burnup-dependent relationships between state variables and the production/consumption of isotopes. Overall, the Q value selected for parameterizing HXS generation models may be different for assorted lattice designs. Using an analysis like the one given above can provide an estimate for the importance of states at earlier burnup steps when predicting HXS at later burnup steps.

4. Sensitivity Results

The following section divided is divided into four subsections. The first of these subsections uses the RHM to report sensitivities of HXS to current and burnup-averaged state variables. The next subsection uses the CHM to demonstrate trends in the significance of the historical states when considering HXS. Next, some analysis is presented that offers guidance on how complex of a history should be considered by looking into the sensitivity of HXS to burnup-averaged state variables. Finally, a section is presented that analyzes how those sensitivities change over burnup. In this section, results for the mean change in HXSs are presented that use the α parameter shown in Equation (3). Again, the following results are included to inform parameterization strategies for modeling approaches to HXS for nodal core simulators. The ranges for which input parameters are sampled from are representative of the domain of models for HXS estimation, as described by Table 1. These domains are not representative of some uncertainty range associated with these state variables as would be the case if this were an uncertainty analysis study.

4.1. Parametric Sensitivity Analysis Using RHM

First, it is useful to understand the sensitivity of HXSs to the various state variables. As mentioned previously, after the standardization transformation is applied to the state vectors, the fitted model coefficients correspond to the SRC measure of sensitivity. To make the results easily interpretable and yield only two sensitivity values for each parameter, the RHM with $Q = 0$ will be used. Table 3 shows these sensitivities for the instantaneous values of the state variables (β_0) as well as the burnup-averaged value of the state variable (γ). To explain, the sensitivity measures indicated by β_0 are measures of the sensitivity of an HXS to the instantaneous value of a particular state variable. Higher values for this measure suggest a stronger influence of either ρ, T_f or b at the time the HXS is calculated on the HXS shown. Sensitivity measures indicated by γ are measures of the sensitivities of an HXS to the historic average value of a particular state variable. Higher values for this measure suggest a stronger influence of history-averaged ρ, T_f or b values on the HXS shown. The dataset described in row 4 of Table 2 that varies in the ρ, T_f and b state variables is used. Burnup values of 9 GWD/MTU ($n = 3$) and 30 GWD/MTU ($n = 10$) for both groups in Σ_f and Σ_{rm} are selected because they can reflect results from early in the irradiation of a lattice to midway through the cycle. Being SRC measures, there is no unit associated with the results. These sensitivity measures can be interpreted as a linear approximation of the change in an HXS with respect to a particular state variable that has been normalized to their respective ranges of variability. Higher numbers indicate that a particular HXS is more strongly influenced by that parameter. The sign of the sensitivity

measure indicates whether a decrease or increase in an HXS is expected for an increase in the state variable.

Table 3. SRC measures for the sensitivity of homogenized fission cross-section (Σ_f) and homogenized removal cross-section (Σ_{rm}) to instantaneous (β_0) and burnup-averaged (γ) values for the coolant density (ρ), fuel temperature (T_f), and boron concentration in coolant (b). Results are calculated using the RHM with Q = 0. Numerical digit subscripts on cross-sections indicate neutron energy group.

		$\Sigma_{f,1}$			$\Sigma_{f,2}$		
		ρ	T_f	b	ρ	T_f	b
$BU_{n=3}$ = 9 GWD/MTU	β_0	0.769	0.110	0.305	0.796	0.125	−0.391
	γ	−0.227	0.156	0.457	−0.172	0.147	0.422
$BU_{n=10}$ = 30 GWD/MTU	β_0	0.714	0.148	0.152	0.325	0.329	−0.327
	γ	−0.235	0.186	0.500	-0.241	0.222	0.628
		$\Sigma_{rm,1}$			$\Sigma_{rm,2}$		
$BU_{n=3}$ = 9 GWD/MTU	β_0	1.000	0.016	−0.002	0.504	0.032	0.812
	γ	−0.001	−0.000	−0.001	0.027	0.017	0.072
$BU_{n=10}$ = 30 GWD/MTU	β_0	1.001	0.016	−0.001	0.480	0.069	0.833
	γ	−0.001	0.001	0.002	−0.038	0.034	0.089

Among the instantaneous parameters (β_0), $\Sigma_{f,1}$ and $\Sigma_{f,2}$ have the largest sensitivity to ρ. This should result from spectral shifts and resonance upscattering near low-lying U-238 absorption resonances. In many reactor systems, there is a large amount of uncertainty in coolant density due to complex flow patterns, heterogeneities in pin power, difficulties for high-fidelity simulation, and more, causing this to be an important parameter in reactor analysis. These uncertainties can lead to a larger effect on the particular HXS than uncertainties in other parameters. These results suggest that, in HXS generation models for fission cross-sections, coolant density may be the parameter with the largest influence. Moving on, boron concentration is shown to have an opposite effect on $\Sigma_{f,1}$ than it does on $\Sigma_{f,2}$. The hardening of the neutron energy spectra from the presence of boron may be an explanation for this behavior. Cross-section homogenization involves a flux-weighted average cross-section over the concerned area and energy range in the lattice. By shifting the neutron energies into higher energies, within the range of the respective group, the smaller macroscopic cross-sections for the higher-energy neutrons will receive greater weights. For $\Sigma_{rm,1}$, the instantaneous ρ has the highest sensitivity. A significant part of $\Sigma_{rm,1}$ involves the downscattering of neutrons from group 1 to group 2, which is dominated by neutron interactions with the light hydrogen atoms in the coolant. For $\Sigma_{rm,2}$, the instantaneous value of ρ has a much smaller relative effect than $\Sigma_{rm,1}$. In this case, $\Sigma_{rm,2}$ is largely composed of thermal neutron absorption where the fuel characteristics have influence. Boron is intentionally used as a thermal neutron absorber so it is expected to have a large effect on $\Sigma_{rm,2}$. It is also important that, for the thermal fission HXS, the sensitivities corresponding to the burnup-averaged state variables can be larger than those corresponding to the instantaneous state variables. This indicates that, in this application of the methodology, it would be important to include history effects in the modeling of Σ_f, particularly for the thermal group.

4.2. Parametric Sensitivity Analysis Using CHM

In this section, analysis is presented on the sensitivity of HXS to the historic values of the state parameters using the CHM. Again, for this analysis, the dataset described in row 4 of Table 2 is used with the standardization transformation, containing variability in the ρ, T_f, and b state variables. For the CHM, sensitivity coefficients can be found for every state parameter at every burnup step during depletion as shown in Figure 5. This results in an understanding of how past values of state variables can effect the value of an

HXS later in life. In this figure, the sensitivity of both groups of Σ_f and Σ_{rm} (as indicated by the legend) is shown for each state variable for two different burnups as a function of past burnup value. Following the notation shown in Figure 2, BU_n corresponds to the burnup of the HXS that the sensitivity is being computed for. In these plots, j is introduced as an integer index to indicate past values of burnup as $BU_j = j\Delta B$. β refers to a general component of $\boldsymbol{\beta}$, and the $n-j$ subscript on β ensures that the subscript follows the notation presented in Equation (3). In this figure, high in magnitude β values indicate the amount of influence that the value of a particular state variable at a particular burnup step has on the HXS at the burnup step shown. The sign of β indicates whether a higher value of that state variable, at that particular burnup step, will lead to a higher, or lower, value for the HXS.

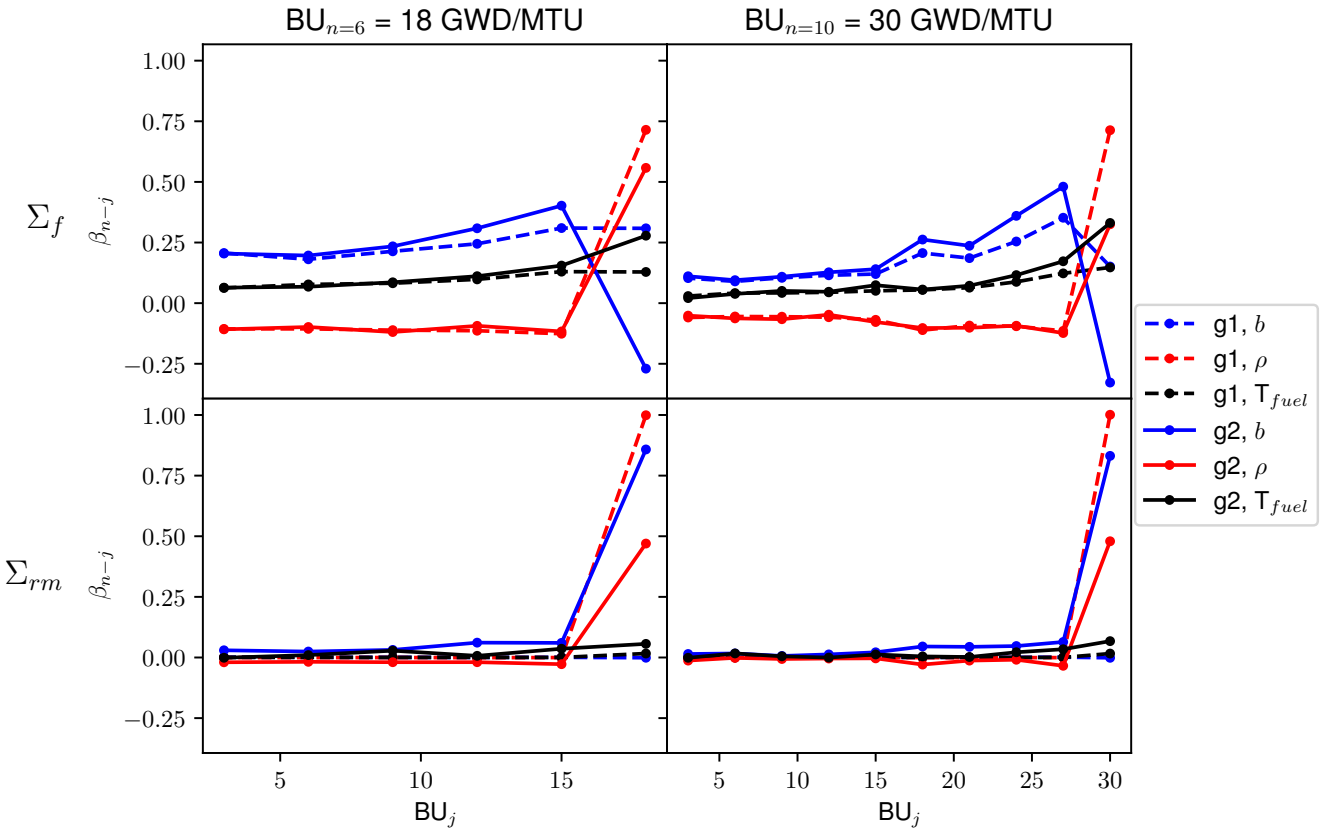

Figure 5. Sensitivity coefficients for previous and current values of state vector $\vec{x}$ for a burnups equal to 18 GWD/MTU and 30 GWD/MTU using the CHM. In the legend, g# indicates the energy group of the HXS for which the sensitivity measure corresponds.

From these results, it is clear that the sensitivities corresponding to the HXS behave differently depending on which reaction is considered. For Σ_f, there is a much stronger dependence on the past values of the state variables. This is indicated by higher β values at lower values of BU_j for the subplots corresponding to the Σ_f cross-section. This seems intuitive because this cross-section is more dependent on the isotopic composition of the fuel which is certainly dependent on the past lattice configuration. From the results for group 2 in Σ_f at $BU_{n=6}$ = 18 GWD/MTU, ρ and b have the largest effect. Interestingly, the sign of the sensitivity coefficient for these state variables changes when moving from the past values of the state variable ($j < n$) to the value of the state variable for which the HXS is calculated ($j = n$). In the case for boron, an explanation for this is that, in conditions with high boron concentration, the neutron spectrum is hardened. With this hardened spectrum, more heavy actinides are generated from U-238 since higher-energy neutrons increase the breeding ratio such that more fissile material is generated. This extra fissile material also decreases U-235 consumption per-unit-burnup (fission of heavy actinides contributes to energy output of lattice), leaving more U-235 to contribute to the

fission cross-section. This is why relatively higher past values of boron concentration increase Σ_f. This fuel composition is carried through irradiation despite the fact that higher boron concentration will reduce the total fission cross-section for group 2. Values of boron concentration that correspond to the step that the HXS is calculated to suppress the group 2 fission cross-section due to its high thermal absorption cross-section. Similar logic can be applied to the trends seen for the sensitivities corresponding to the coolant density parameter. Lower coolant densities harden the neutron spectrum, causing more U-235 to remain per-unit-burnup. However, lower coolant densities in the lattice at the time in which the cross-section is calculated lowers the fission cross-section. Again, as observed in Table 3, there seems to be a smaller dependence of Σ_{rm} on past state variable values. This is indicated by lower β values at lower values of BU_j for the subplots corresponding to the Σ_{rm} cross-section. There is less dependence of the removal cross-section on the fuel composition which explains why the configuration of the lattice in its irradiation history would matter less.

4.3. Burnup-Averaged State Variable Importance

Another useful result that can be obtained with the RHM is quantifying the sensitivity of the HXS to burnup-averaged values of state variables. This allows for a determination of the importance of the historical values of a state variable in creating models to predict HXS. Figure 6 shows the γ parameter from the RHM as a function of the burnup-averaging threshold for Σ_f. The BU_Q axis can be interpreted as the last value of the state variable that is averaged in the history before assigning each state variable its own β fitted parameter, or, in terms of the variables given in Equation (4), $BU_Q = Q\Delta B$, where Q is the reduction parameter used to create the model. Each point in Figure 6 corresponds to a separate model fit by OLS. Only Σ_f is shown because of its increased sensitivity to the historical configuration of the lattice. The y-axis, labeled γ, on these plots can be interpreted as the importance of the burnup-averaged values of the state variables as more state variables are included in the averaging. As more lattice states are included, naturally, the influence of the average of these lattice states on the HXS at some later burnup grows. These plots can be used to inform a parameterization approach to HXS generation because they can be used to identify how much is being lost for a particular selected Q value, based on the magnitude of γ at some BU_Q. The analysis done in this section uses the same dataset as the one used in Section 4.2.

As expected, the sensitivity of Σ_f to the burnup-averaged values of the state variables increases as more burnup steps are averaged. This is indicated by increasing γ values as BU_Q increases. Across all state variables and burnups shown, this trend does not seem to be linear for the latter portions of the plots. Instead, as burnup steps are included in the averaged quantity, there is a non-constant increase in the sensitivity. This trend can be explained by the nonuniformity in the sensitivity of HXS to each past value of the state variable as shown in Figure 5. For burnup steps sufficiently close to the burnup at which the HXS is calculated, the values of state variables closer to the burnup for which the HXS is calculated are more important than the historical values of those state variables. This is shown by the increasing values of β for larger values of BU_j in this figure. The results from Figure 5 do seem to suggest that there is some threshold where the state variables go from having equal importance to having increasing importance, and this observation is confirmed separately with more burnup steps than those shown in the figure. This threshold may provide some reasonable criteria for an analyst to select some Q. Algebraically, assigning a single fitted parameter to a burnup-averaged quantity is identical to assigning the same fitted parameter to multiple states of a burnup-dependent quantity. Therefore, selecting Q such that all of the burnup-averaged state variables have roughly equal sensitivity will result in a relatively small loss of model accuracy. This conclusion can be used in more complex model creation to asses how historical values of the state variables are treated.

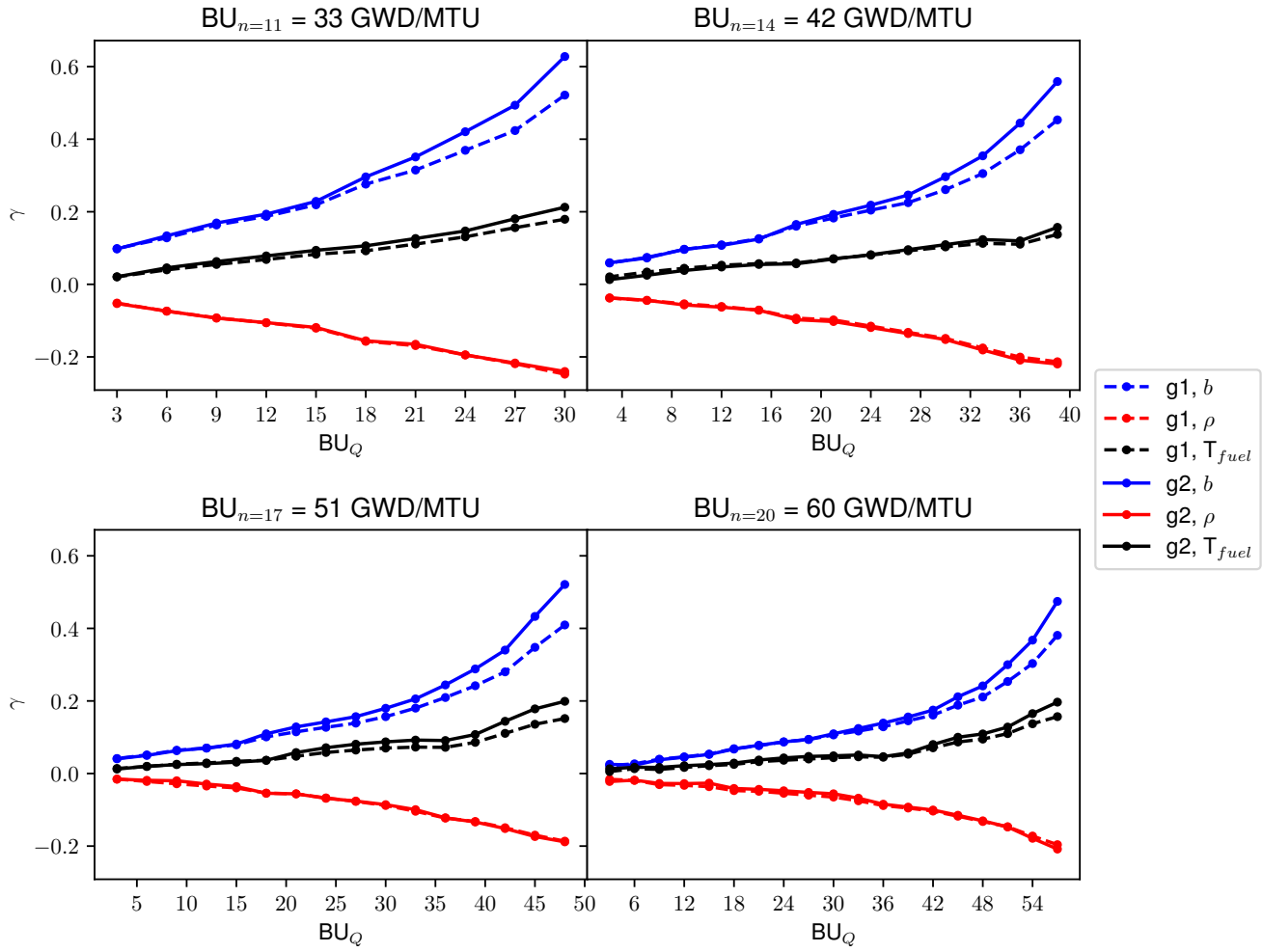

Figure 6. Sensitivities of Σ_f to burnup-averaged values of state variables. Subfigure headers correspond to the burnup at which the HXS is calculated. In the legend, g# indicates the energy group of the HXS for which the sensitivity measure corresponds.

In addition, when considering both Figures 5 and 6, there is little difference in the trend of sensitivities associated with group 1 and group 2 cross-sections for historical values of state variables. An explanation for this is that the historical effects exist solely due to differences in the isotopic composition of the fuel. These differences in fuel isotopic composition should affect both groups of the HXS similarly. To explain, if we consider the simplest form of an HXS, that being one associated with a homogeneous medium of a single isotope, we know that the macroscopic cross-section is a product of the energy-dependent microscopic cross-section associated with the isotope and the number density of that isotope. Regardless of the energy dependence of the microscopic cross-section, the macroscopic cross-section will be linearly dependent on the number density of the isotope. In considering the more complicated lattice system, historical values of the state variables will essentially act as perturbations to the number densities associated with the isotopes in the lattice fuel. These perturbations will manifest themselves as linear increases/decreases in the HXS that will be proportional to the microscopic cross-section corresponding to that isotope at a given neutron energy.

4.4. Stationarity Analysis

As a lattice produces energy, the isotopic composition of the fuel changes as a function of amount of energy produced. Clearly, this means that the HXSs change during burnup, resulting in a nonstationary process. Simple analysis methods may select some nominal depletion conditions and perform a lattice burnup calculation and track the change in

HXS as a function of burnup. However, this method fails to account for the range of possible operating conditions a reactor can undergo and the selected nominal states may not necessarily be representative of the mean behavior of the HXS during depletion. Using the models presented in the current study, one can capture the mean behavior of the HXS during burnup using the scaling parameter, α, shown in Equation (4). In order to perform this analysis properly, the state vectors should undergo a standardization transformation, but the code-calculated HXS should not so the α term represents the HXS when all state variables sit at their mean values (0 after the standardization transformation). Figure 7 shows the result of using such an analysis on the same dataset as Section 4.2. In this figure, α indicates the mean behavior of a cross-section for some burnup BU_n across the state variable ranges considered for the standardized set of variables. For specific applications, the standardization transformation can not be applied to the HXS in question to obtain dimensionalized values for this sort of analysis. In general, the trends shown are well understood in the reactor-physics community. For example, an increasing removal cross-sections arises because of the increasing number of fission products accumulating in the lattice and the decreasing fission cross-sections come about because of the consumption of fissile material in the lattice. From a sensitivity approach, the results shown can be used to determine the sensitivity of an HXS to burnup levels by looking at the slope of the line at a particular burnup.

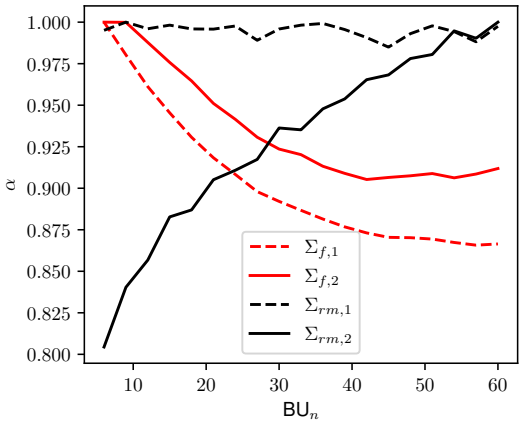

Figure 7. Mean behavior of HXS during burnup using α parameter from Equation (4). α demonstrates an estimation for the behavior of the HXS if all state variables were set to their mean value over the entire history.

Furthermore, it can be useful to analyze the change of sensitivities during burnup. This can be used to evaluate the degree to which a model created to predict HXSs for some reactor configurations at some burnup may be valid for predicting HXSs at other burnups. For some reactor designs, it may be possible that these sensitivities do not change over burnup, which may greatly reduce the need to characterize the effect of perturbations to of deep-burnup reactor states when creating models for HXS prediction. However, as shown in Figure 8, this is not the case for the current application. In this figure, estimates for the sensitivity of both energy groups of Σ_f to the various state variables is shown as a function of burnup. Sensitivities to both burnup-averaged and instantaneous values of the state variables are calculated using the RHM with $Q = 0$. In this figure, the label "SRC" is used to refer to the more general standardized regression coefficient of which β_0 and γ are specific instances. The sensitivities of Σ_f to the instantaneous state variables remains more constant than those to the burnup-averaged state variables, particularly for group 1. Regardless, there is variation in these sensitivities. This suggests that conventional branching calculations, where the effect of perturbations to state variables at multiple points during a burnup in a nominal configuration, are certainly warranted to capture the changing sensitivity over burnup. However, this branching method from a nominal

depletion state may not capture the history effects appropriately unless other depletion states are considered (which they often are [28]). Moving on, these results suggest that perturbations to burnup-averaged state variables have a larger effect on Σ_f as burnup increases. This can be justified by the fact that—on average—the reactor would be spending a longer time in the perturbed state which would magnify the effect of the perturbation on the isotopic composition of the fuel. This larger deviation in fuel composition from the composition at a nominal state should exaggerate the system's sensitivity to those burnup-averaged quantities.

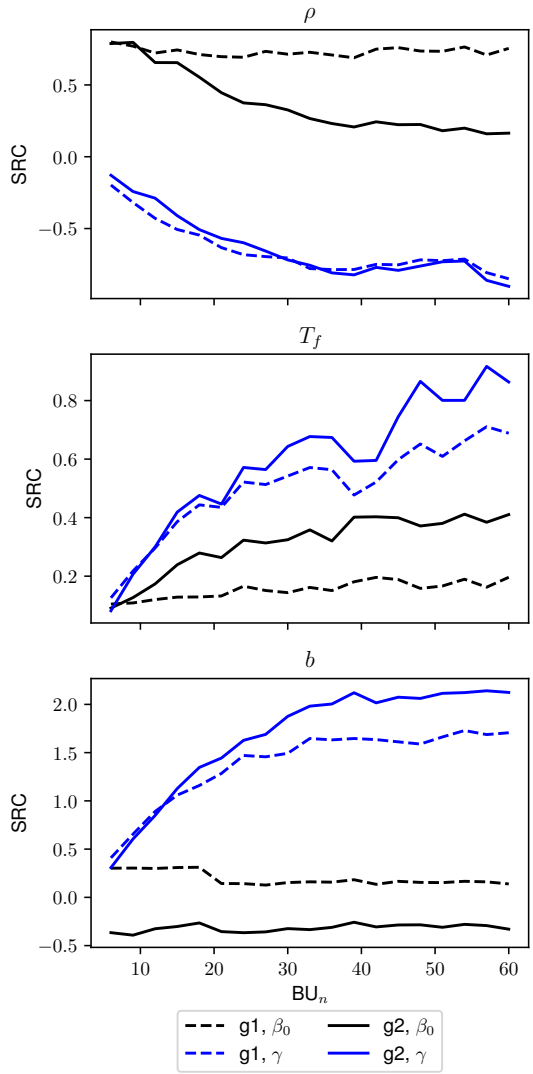

Figure 8. Sensitivity measures for both groups of Σ_f from the SRC method for both burnup-averaged state variables (γ) and state variables at the burnup where the HXS is calculated (β_0) as a function of burnup. Sensitivity measures calculated at each burnup step using the RHM where Q = 0. In the legend, g# indicates the energy group of the HXS for which the sensitivity measure corresponds.

5. Conclusions

This paper presents a methodology that may inform parameterization of the homogenized cross-section estimation process for application in the two-step method for reactor simulation. This methodology presents sensitivities of HXS to both state variables for the configuration at which the HXS is calculated and sensitivities to state variables of past reactor configurations. These sensitivities are largely derived from the SRC method [29] where instantaneous, historical, and burnup-averaged state variables are the parameters of interest. Two models for sensitivity estimation are presented:

- Full History Model (FHM): Uses every reactor state variable in the history leading up to the burnup at which the HXS is calculated to calculate sensitivities.
- Reduced History Model (RHM): Uses a reduction parameter to use burnup-averaged state variable values instead of considering the reactor state at every burnup step.

Both models present a sensitivity estimate that is local in burnup, in that the response of HXS to perturbations is estimated for every burnup step, and global with respect to the state variables. Thus, responses of HXS to perturbations are uniform for every reactor configuration within a burnup step. These models also rely on the linearity of the relationship between the HXS and the state variables, which can be evaluated within this methodology using the techniques shown in Section 3.

An application of this methodology on a 17 × 17 lattice for the Westinghouse AP1000® reactor is presented where coolant density, fuel temperature, boron concentration in coolant, and control rod insertion are the state variables of interest. It was found that the linearity assumption was accurate over the domain of state variables chosen. Furthermore, it was found that fitting an RHM that only considers the burnup-averaged values of the state variables and value of the state variable at the time that the HXS is calculated can lead to notable losses in model accuracy as shown in Figure 4. The HXSs used in this application are the 2-group fission cross-section and the 2-group removal cross-section, but the methodology is certainly applicable to any other energy structure or reaction type. It was found that the historical values of state variables had a much larger effect on the fission cross-sections than the removal cross-sections. In addition, across all cross-sections considered, the fuel temperature seemed to have the least influence. A demonstration of the dependence of these sensitivities on burnup was also given, with the result that the instantaneous values of the state variables have a more constant sensitivity over burnup as compared to burnup-averaged quantities. Future work will include an application of this methodology to a broader set of LWR lattice designs and potentially advanced reactor designs. It is thought that the presence of burnable absorbers may significantly change these sensitivities due to the complex lattice behavior they introduce. Therefore, performing this sort of analysis on a broader set of LWR lattice designs may offer insight on the differences between lattices with—and without—burnable absorbers.

Author Contributions: D.P.: Methodology, Visualization, Writing—original draft. T.F.: Data curation, Investigation. M.D.: Conceptualization, Writing—review and editing. K.G.: Conceptualization, Supervision, Funding acquisition. B.K.: Conceptualization, Supervision, Writing—review and editing, Funding acquisition. All authors have read and agreed to the published version of the manuscript.

Funding: This material is based upon work supported by the National Science Foundation Graduate Research Fellowship under Grant No. DGE 1256260. We also would like to acknowledge the support of NSF DMREF Grant No.1729166 (M.D. and K.G.) and an interdisciplinary mini-grant from the Fastest Path to Zero Initiative.This material is also based upon work supported under an Integrated University Program Graduate Fellowship.

Institutional Review Board Statement: Not applicable.

Informed Consent Statement: Not applicable.

Data Availability Statement: Not applicable.

Conflicts of Interest: The authors declare no conflict of interest.

References

1. Stamm'ler, R.J.; Abbate, M.J. *Methods of Steady-State Reactor Physics in Nuclear Design*; Academic Press London: London, UK, 1983; Volume 111.
2. Choi, S.; Smith, K.S.; Kim, H.; Tak, T.; Lee, D. On the diffusion coefficient calculation in two-step light water reactor core analysis. *J. Nucl. Sci. Technol.* **2017**, *54*, 705–715. [CrossRef]
3. Knott, D.; Yamamoto, A. Lattice physics computations. In *Handbook of Nuclear Engineering*; Springer Science & Business Media: New York, NY, USA, 2010.
4. Cetnar, J. General solution of Bateman equations for nuclear transmutations. *Ann. Nucl. Energy* **2006**, *33*, 640–645. [CrossRef]

5. Leppänen, J.; Pusa, M.; Viitanen, T.; Valtavirta, V.; Kaltiaisenaho, T. The Serpent Monte Carlo code: Status, development and applications in 2013. *Ann. Nucl. Energy* **2015**, *82*, 142–150. [CrossRef]
6. Rearden, B.T.; Jessee, M.A. *SCALE Code System*; Technical Report; Oak Ridge National Laboratory (ORNL): Oak Ridge, TN, USA, 2016.
7. Rhodes, J.; Smith, K.; Lee, D. CASMO-5 development and applications. In Proceedings of the PHYSOR-2006 Conference, ANS Topical Meeting on Reactor Physics (Vancouver, BC, Canada, 2006) B, Vancouver, BC, Canada, 10–14 September 2006; Volume 144.
8. Kochunas, B.; Collins, B.; Jabaay, D.; Downar, T.J.; Martin, W.R. Overview of development and design of MPACT: Michigan parallel characteristics transport code. In Proceedings of the 2013 International Conference on Mathematics and Computational Methods Applied to Nuclear Science and Engineering-M and C 2013, Sun Valley, ID, USA, 5–9 May 2013.
9. Park, H.J.; Shim, H.J.; Joo, H.G.; Kim, C.H. Generation of few-group diffusion theory constants by Monte Carlo code McCARD. *Nucl. Sci. Eng.* **2012**, *172*, 66–77. [CrossRef]
10. Smith, K.S. Assembly homogenization techniques for light water reactor analysis. *Prog. Nucl. Energy* **1986**, *17*, 303–335. [CrossRef]
11. Downar, T.; Xu, Y.; Seker, V.; Hudson, N. *Theory Manual for the PARCS Kinetics Core Simulator Module*; Department of Nuclear Engineering and Radiological Sciences University of Michigan: Ann Arbor, MI, USA, 2009.
12. Smith, K. *SIMULATE-3: Advanced Three-Dimensional Two-Group Reactor Analysis Code*; STUDSVIK/SOA-8904; Studsvik of America: Atlanta, GA, USA, 1989 .
13. Botes, D.; Bokov, P.M. Polynomial interpolation of few-group neutron cross sections on sparse grids. *Ann. Nucl. Energy* **2014**, *64*, 156–168. [CrossRef]
14. Sánchez-Cervera, S.; García-Herranz, N.; Herrero, J.; Cabellos, O. Optimization of multidimensional cross-section tables for few-group core calculations. *Ann. Nucl. Energy* **2014**, *69*, 226–237. [CrossRef]
15. Botes, D.; Bokov, P.M. Hierarchical, multilinear representation of few-group cross sections on sparse grids. In Proceedings of the M&C 2011: International Conference on Mathematics and Computational Methods Applied to Nuclear Science and Engineering, Rio de Janeiro, Brazil, 8–12 May 2011; Volume 48.
16. Zimin, V.G.; Semenov, A.A. Building neutron cross-section dependencies for few-group reactor calculations using stepwise regression. *Ann. Nucl. Energy* **2005**, *32*, 119–136. [CrossRef]
17. Bokov, P.M. Automated few-group cross-section parameterization based on quasi-regression. *Ann. Nucl. Energy* **2009**, *36*, 1215–1223. [CrossRef]
18. Szames, E.; Tomatis, D. A review of history parameters in PWR core analysis. *Nucl. Eng. Des.* **2019**, *347*, 158–174. [CrossRef]
19. Mosteller, R. Impact of moderator history on physics parameters in pressurized water reactors. *Nucl. Sci. Eng.* **1988**, *98*, 149–153. [CrossRef]
20. Fujita, T.; Endo, T.; Yamamoto, A. A macroscopic cross-section model for BWR pin-by-pin core analysis. *J. Nucl. Sci. Technol.* **2014**, *51*, 282–304. [CrossRef]
21. Tomatis, D.; Galia, A.; Pastoris, S.; Zmijarevic, I. Quantification of history effects in PWR modelling. *Nucl. Eng. Des.* **2017**, *325*, 205–217. [CrossRef]
22. Ivanov, K.; Avramova, M.; Kamerow, S.; Kodeli, I.A.; Sartori, E.; Ivanov, E.; Cabellos, O. *Benchmark for Uncertainty Analysis in Modeling (UAM) for Design, Operation and Safety Analysis of LWRs*; Citeseer: Issy-les-Moulineaux, France , 2013; Volume 1.
23. Gentry, C.; Godfrey, A.T.; Franceschini, F. AP1000®Benchmarking of VERA Neutronics Toolset. In Proceedings of the M&C 2017: International Conference on Mathematics and Computational Methods Applied to Nuclear Science and Engineering, Jeju, Korea, 16–20 April 2017.
24. Downar, T.; Collins, B.S.; Gehin, J.C.; Godfrey, A.T.; Jabaay, D.; Kelley, B.W.; Clarno, K.T.; Kim, K.; Kochunas, B.; Larsen, E.W.; et al. *MPACT Theory Manual, Version 2.2.0*; Technical Report; Oak Ridge National Laboratory (ORNL) : Oak Ridge, TN, USA, 2016.
25. Turner, J.A.; Clarno, K.; Sieger, M.; Bartlett, R.; Collins, B.; Pawlowski, R.; Schmidt, R.; Summers, R. The virtual environment for reactor applications (VERA): Design and architecture. *J. Comput. Phys.* **2016**, *326*, 544–568. [CrossRef]
26. Luu, T.H.; Maday, Y.; Guillo, M.; Guérin, P. A new method for reconstruction of cross-sections using Tucker decomposition. *J. Comput. Phys.* **2017**, *345*, 189–206. [CrossRef]
27. Bokov, P.M.; Botes, D.; Zimin, V.G. Pseudospectral Chebyshev representation of few-group cross sections on sparse grids. In Proceedings of the International Conference PHYSOR, Knoxville, TN, USA, 15–20 April 2012 ; pp. 15–20.
28. Cacuci, D.G. *Handbook of Nuclear Engineering: Vol. 1: Nuclear Engineering Fundamentals; Vol. 2: Reactor Design; Vol. 3: Reactor Analysis; Vol. 4: Reactors of Generations III and IV; Vol. 5: Fuel Cycles, Decommissioning, Waste Disposal and Safeguards*; Springer Science & Business Media: New York, NY, USA, 2010.
29. Schielzeth, H. Simple means to improve the interpretability of regression coefficients. *Methods Ecol. Evol.* **2010**, *1*, 103–113. [CrossRef]